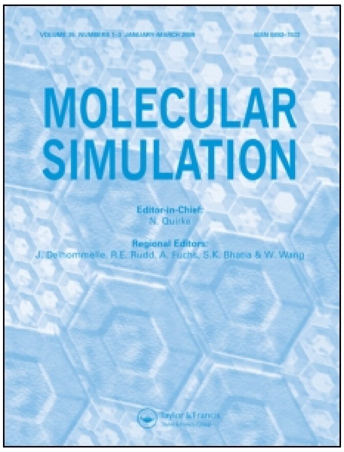

Molecular Simulation

Publication details, including instructions for authors and subscription information:
http://www.informaworld.com/smpp/title~content=t713644482

Simulation and Characterization of the Structure of Vitreous Silica

B. Vessal[a]; M. Amini[b]; C. R. A. Catlow[c]
[a] Catalysis and Sorption Project, Biosym Technologies, San Diego, CA, USA [b] Department of Physics, Isfahan University of Technology, Isfahan, Iran [c] The Royal Institution of Great Britain, London, UK

To cite this Article Vessal, B. , Amini, M. and Catlow, C. R. A.(1995) 'Simulation and Characterization of the Structure of Vitreous Silica', Molecular Simulation, 15: 2, 123 — 134

To link to this Article: DOI: 10.1080/08927029508022333

URL: http://dx.doi.org/10.1080/08927029508022333

Molecular Simulation, 1995, Vol. 15, pp. 123–134
Reprints available directly from the publisher
Photocopying permitted by license only

SIMULATION AND CHARACTERIZATION OF THE STRUCTURE OF VITREOUS SILICA

B. VESSAL

Catalysis and Sorption Project, Biosym Technologies, 9685 Scranton Road,
San Diego, CA 92121, USA

M. AMINI

Department of Physics, Isfahan University of Technology, Isfahan, Iran

C. R. A. CATLOW

The Royal Institution of Great Britain, 21 Albemarle Street,
London, W1X 4BS, UK

(Received January 1995, accepted March 1995)

Atomistic computer simulation methods can yield unique insights into the structural properties of glasses. In this paper we report on the simulation of vitreous silica employing three-body terms and the subsequent characterization of the structure using ring statistics, and Voronoi Polyhedra.

KEY WORDS: Molecular dynamics, vitreous, silica, amorphous, glass, Voronoi Polyhedra

1 INTRODUCTION

The major thrust in the last ten years in the field of computer simulation of condensed matter has been towards realistic simulations of systems of increasing complexity. Indeed, computer simulation methods are now able to make accurate predictions of the atomistic properties of systems as diverse as zeolite catalysts [1] and DNA [2]. Amorphous materials present one of the greatest challenges to the applications of such techniques. Experimental methods cannot at present yield accurate structures at the atomic level: they give averaged structures as in the Radial Distribution Functions (RDFs) provided by diffraction measurements, or very local information as in Extended X-ray Absorption Fine Structure (EXAFS) and Nuclear Magnetic Resonance (NMR) experiments; knowledge on intermediate level order is sparse. Computer modelling techniques have, however, the opportunity of yielding detailed models for the structures of amorphous materials at the short and intermediate level.

In this paper we will show how it is possible to model the structure of vitreous silica which give accurate agreement with experimental diffraction data, and subsequently characterize the structure using ring statistics and Voronoi polyhedra analysis.

2 COMPUTATIONAL DETAILS

In this section we give the details of the interatomic potentials and the detailed methodology that was employed in our simulation of vitreous silica.

The long range coulomb part of the potential is calculated using Ewald's method [3], and employing full ionic charges on both the silicons and the oxygens. Following Sangster and Dixon [4], and Anastasiou and Fincham [5] we write the coulomb part of the potential as follows:

$$E^c = E_1^c + E_2^c + E_3^c \tag{1}$$

$$E_1^c = \sum_{\substack{i=1\\ i>j}}^{N} \sum_{j=1}^{N} Z_i Z_j \operatorname{erfc}(\alpha r_{ij})/r_{ij} \tag{2}$$

$$E_2^c = \sum_{i=1}^{N} Z_i^2 \alpha \pi^{-1/2} \tag{3}$$

$$E_3^c = \sum_{i=1}^{N} \sum_{\mathbf{k}=\mathbf{0}} A(k)\left[\left(\sum_{j=1}^{N} Z_j e^{i\mathbf{k}.\mathbf{r}_j}\right) Z_i e^{-i\mathbf{k}.\mathbf{r}_i}\right] \tag{4}$$

where E_1^c and E_2^c are known as the direct and the reciprocal lattice parts of the coulomb energy respectively. N is the number of ions in the simulation box, Z_i and Z_j are the charges on the ions i and j, r_{ij} is the distance between i and the nearest image of j, and α is called the Ewald parameter. The choice of this parameter determines the value of the direct and reciprocal sum cutoffs. If one wishes to determine the direct and reciprocal lattice sums to an accuracy A_c, then the value of the direct lattice cutoff that is used is $r_{\max} = f/\alpha$, and the reciprocal lattice cutoff is $k_{\max}/2\pi = \alpha f/\pi$, where $f = (-\ln A_c)^{1/2}$. We used a value of α that gives comparable number of terms in both the direct and reciprocal lattice sums, i.e.,

$$\alpha = (N\pi^3/V^2)^{1/6} \tag{5}$$

where V is the volume of the simulation box.

The sum over $\mathbf{k}$ need only be carried out over half of reciprocal space and the final result doubled since reciprocal space is always centrosymmetric. Thus the z component of the reciprocal lattice vector will always be taken as positive.

In Equation (4) $\mathbf{k}$ is 2π times a reciprocal lattice vector and $\mathbf{r}$ is an atom position. The maximum number of reciprocal lattice vectors in the x, y and z directions N_x, N_y, N_z are determined from the formula given below:

$$N_x = (\mathbf{k}_{\max}/2\pi)|\mathbf{l}_x| \tag{6}$$

where $\mathbf{l}_x$ is the x column of a matrix whose columns are the unit cell lattice vectors. $A(\mathbf{k})$ is defined as

$$A(\mathbf{k}) = 2\pi/V \exp(-k^2/4\alpha^2)/k^2 \tag{7}$$

We have not included the $\mathbf{k} = \mathbf{0}$ term in our calculations.

A four range Buckingham potential is used to model the short range interactions between different ions.

$$E_{ij} = A_{ij}\exp(-r_{ij}/\rho_{ij}), \quad r_{ij} < r_1 \tag{8}$$

$$E_{ij} = \sum_{m=0}^{5} A_m r_{ij}^m, \quad r_1 < r_{ij} < r_2 \tag{9}$$

$$E_{ij} = \sum_{m=0}^{3} B_m r_{ij}^m, \quad r_2 < r_{ij} < r_3 \tag{10}$$

$$E_{ij} = -C_{ij}/r_{ij}^6, \quad r_3 < r_{ij} < r_c \tag{11}$$

where r_c is the short range cutoff. We have used a value of 7.6 A for r_c.

The function is splined at r_1, r_2, and r_3 so that the energy, and first and second derivatives are continuous. The function has a minimum at r_2. Despite the complex nature of the potentials, we are able to fit the different components using a cubic spline which is then used in the forces calculation.

A cubic spline is either fitted separately to the Coulomb direct space error function term and to the short range potential, or to the sum of the two terms. Two separate splines are needed if pressure is to be calculated. One thousand points are used in the spline. The spline is fitted to the square of the distance to avoid calculating a square root.

An essential feature of our potential model is the inclusion of two different types of three-body potentials, one between the O–Si–O triads and the other between Si–O–Si triads. Consider the three atoms i, j, and k interacting according to the following potential:

$$E_{ijk} = k_{ijk}[\theta^n(\theta-\theta_0)^2(\theta+\theta_0-2\pi)^2 - n/2\pi^{n-1}(\theta-\theta_0)^2(\pi-\theta_0)^3] \tag{12}$$

and where k_{ijk} is the three-body spring constant and θ_0 is the equilibrium bond angle, i.e. 109°28′ in the case of O–Si–O interactions and 144° for Si–O–Si interactions, and θ is the calculated bond angle.

The parameters for the short-range and three-body potentials are determined using the THBFIT code which uses a least-squares fitting method to get the best agreement between the observed and the computed properties of α-quartz.

3 RESULTS AND DISCUSSION

Simulated glass structures are prepared computationally in the same way as real glasses. Models of crystalline systems are melted; the melts are then quenched freezing the structure into a disordered glassy phase. The main problem with this technique is in the time scale of the melting and more particularly of the quench, as with current computational capabilities, these are several orders of magnitude greater than the rates achieved experimentally. As a consequence, simulated glass structures have very high fictive temperatures. Nevertheless, the information obtained on glass structures is of great value.

We recently reported on the development of a potential model [6] which gives a good representation of the structural and dielectric properties of crystalline SiO_2, and could be successfully implemented in a quenched MD simulation of the amorphous material. It works well for high temperature and high pressure melts. The model has been used extensively, with applications to the melting of β-cristobalite [7–8], where 'water-like' melting behavior was predicted in agreement with experiment [9], and to the modelling of the dynamical properties of zeolite pores [10–11]. The same potential has also been employed in the study of a range of alkali silicate glasses [12], the pressure amorphisation of α-quartz [13], titanium and zirconium wadeites [14] and simulation of molten silica at high pressure [15].

Despite the general success of this model, we have found inadequacies in describing the RDF of vitreous silica. We have therefore developed an improved potential details of which are given elsewhere [16], and which yields a highly accurate structure for the amorphous material, as shown by comparison with RDFs obtained from recent high quality neutron scattering data [17]. We should stress that the information concerning the amorphous structure is not built into our potential which is derived solely from the properties of the crystalline phase.

The simulation of vitreous silica is undertaken at constant volume starting from a molten silica configuration with the experimental density of vitreous silica at 7000 K. A cubic simulation box with periodic boundary conditions is used containing 216 Si^{4+} and 432 O^{2-} ions. The interatomic potentials used in this simulation are listed in Table 1.

After 2000 steps of equilibration, a cyclic procedure is used to cool the melt down to 300 K. Each cycle has a period of 2000 steps. The velocities are scaled for the first 800 steps of each cycle to change the temperature of the system, T, to the target temperature, T_0. During the first 400 steps of each cycle T is calculated from the value of the velocity at each step, while during the second 400 steps of the cycle T is calculated from the average values of velocities over the past 20 steps.

During the remaining 1200 steps of each cycle the system remains undisturbed (no adjustment to T), and all of the physical properties in a cycle are accumulated during

Table 1 Potential parameters for simulation of vitreous silica

Parameter	*Si–O potential*	*O–O potential*	*Units*
A_{ij}	990.6170	4511887.2	eV
ρ_{ij}	0.3297	0.149	Å
C_{ij}	25.0	52.12	eVÅ^6
r_1	1.5	2.9	Å
r_2	2.5	3.6	Å
r_3	3.5	4.2	Å
r_c	7.6	7.6	Å
k_{ijk}(O–Si–O)	0.5		eVrad$^{-5.2}$
k_{ijk}(Si–O–Si)	0.25		eVrad^{-8}
n(O–Si–O)	1.2		
n(Si–O–Si)	4.0		

this period. The properties that are calculated are the average internal energy (U), the temperature, the pressure, the mean square displacements (MSDs), as well as the radial distribution functions (RDFs), and the bond angle distributions (BADs). The total time for annealing of vitreous silica in this case is 36ps. A time-step of 1 fs is employed.

In this simulation the three-body interactions are limited to a maximum of four nearest oxygen neighbors within a cutoff of 3.2 A in the case of silicons, and to a maximum of two nearest silicon neighbors within the same cutoff in the case of oxygens. The RDFs and BADs that are obtained for the vitreous system are shown in Figure 1 and Figure 2 respectively.

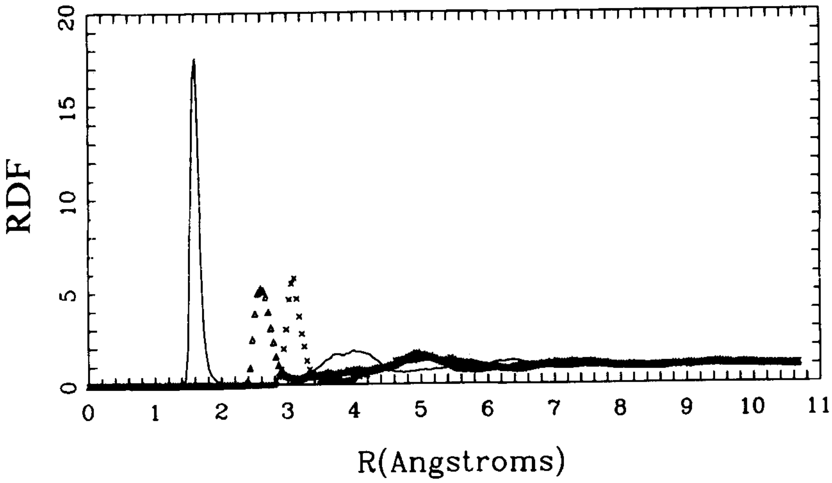

Figure 1 RDF for vitreous silica: ——, Si–O; Δ, O–O; x, Si–Si.

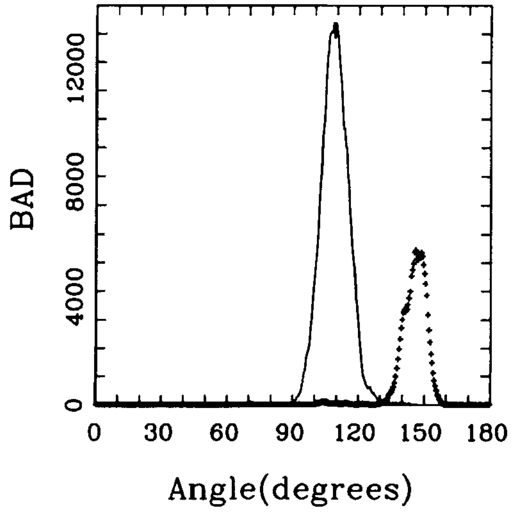

Figure 2 BAD for vitreous silica: ——, O–Si–O; x, Si–O–Si.

A computer generated structure for vitreous silica is shown in Figure 3. It is generally found that MD studies of glassy materials result in a glass structure with a high fictive temperature due to the rapid cooling rates employed. Glass transition temperatures are typically high by a factor of 2. Nevertheless, the structures generated agree well with experiment. Thus, the total radial distribution function obtained for vitreous silica using our potential model is compared with neutron diffraction results in Figure 4, and shows remarkable agreement with the experimental results [17]. Indeed, Wright [18] has compared our model to other models and finds it more accurate than the Bell and Dean model [19].

Since our model gives an accurate representation of the short-range structure of vitreous silica, we can analyze the medium-range structure of the simulated glass. Figure 5 shows the ring analysis for the vitreous silica structure. There is one three-membered ring in the structure. Galeener [20] has assigned the D2 peak ($606\,\mathrm{cm}^{-1}$) in the Raman spectrum of vitreous silica to an oxygen breathing mode in rings of three SiO_4 tetrahedra. This assignment has been reconfirmed recently by Kubicki and Sykes [21] who carried out ab initio molecular orbital calculations to determine the structure and vibrational frequencies of the three-membered ring. The maximum in the figure is for six-membered rings. The topology of the four-membered rings are shown in Figure 6.

One of the useful methods of characterizing an amorphous structure is the use of Voronoi polyhedra. A Voronoi polyhedron is the analog of the Wigner-Seitz cell of solid state physics applied to amorphous solids or liquids. The Voronoi polyhedron surrounding any given atom is the smallest polyhedron formed by the planes which perpendicularly bisect the lines joining the atom to its neighbors. The value of this

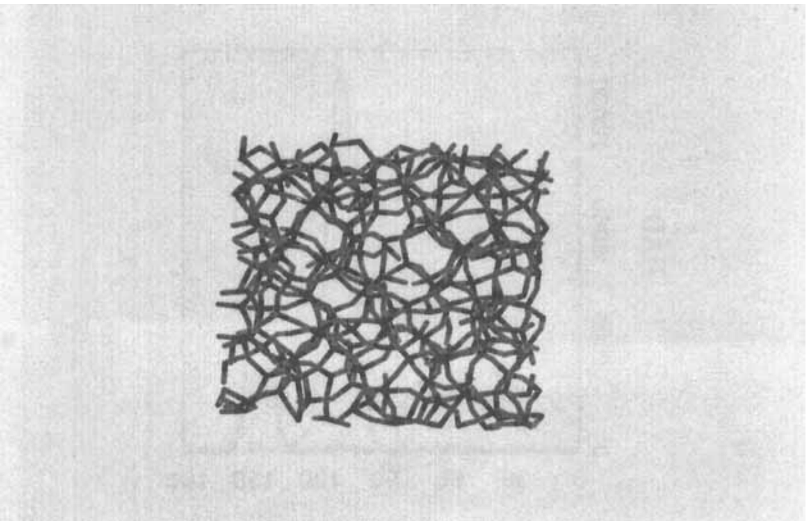

Figure 3 Structure of vitreous silica generated by quenching of molecular dynamics simulated molten SiO_2. Silicons are shown in yellow and oxygens in red. See Color Plate I.

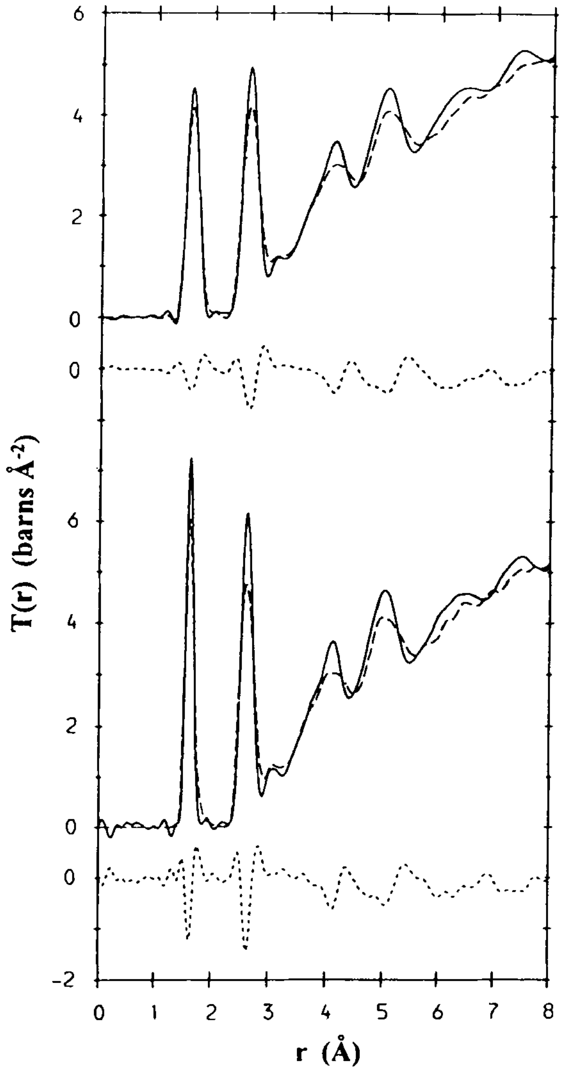

Figure 4 Experimental (————), calculated (— — —), and difference curve (-------) RDF for silica glass. The lower curves are comparison with experimental data in reference [17], while the upper curves are comparison with the more recent data of Wright and co-workers. [23]

concept is that the statistical distribution of quantities such as polyhedron volumes, number of faces per polyhedron, and the number of edges per face constitutes a description of the amorphous structure. We have used the Amorphous_Cell Module of BIOSYM Polymer software to calculate the Voronoi statistics for vitreous silica. The algorithm used for these calculations is that of Tanemura and coworkers [22]. The results are presented in Figures 7–10. The quantity plotted in Figure 9 is a measure of

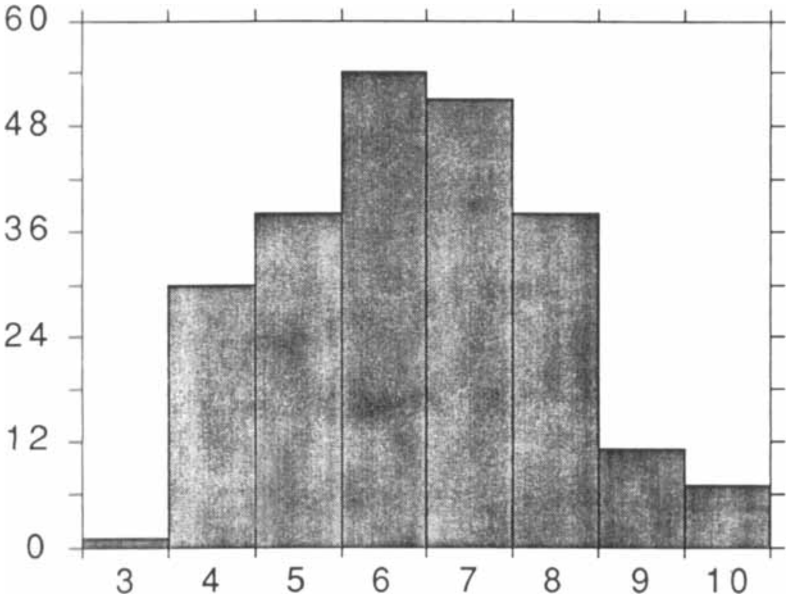

Figure 5 Ring analysis for the computer generated vitreous silica.

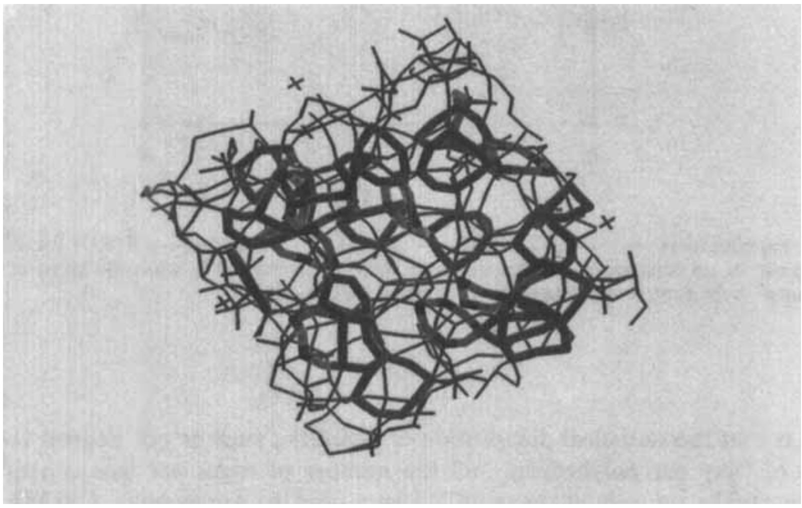

Figure 6 Topology of four-membered rings in vitreous silica. The structure of vitreous silica is shown in purple. The unique four-membered rings are shown in green. The rings sharing corners or edges with other rings are shown in atomic colors. (Yellow for silicons and red for oxygens). See Color Plate II.

asphericity of the polyhedra and is defined as

$$\omega = (S/4\pi)/(3V/4\pi)^{2/3} \tag{13}$$

where S is the surface area and V is the volume. ω has a value of one for a sphere and a value greater than one for aspherical objects. The long tail in the volume plot is due to edge effects. It should be noted that the results that are presented in Figures 7–10 were

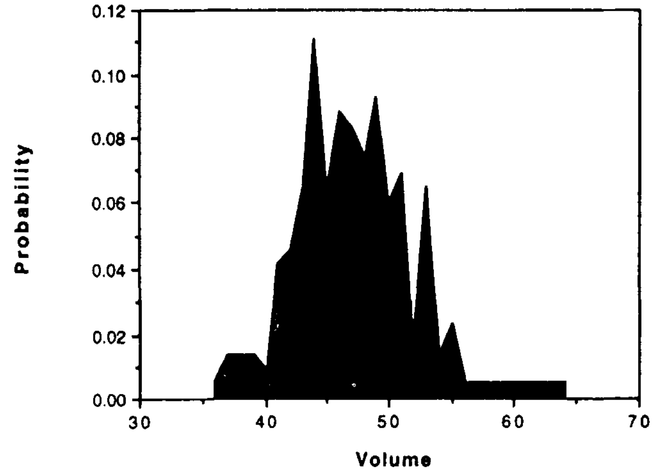

Figure 7 Distribution of volume (Å^3) of the Voronoi polyhedra for vitreous silica.

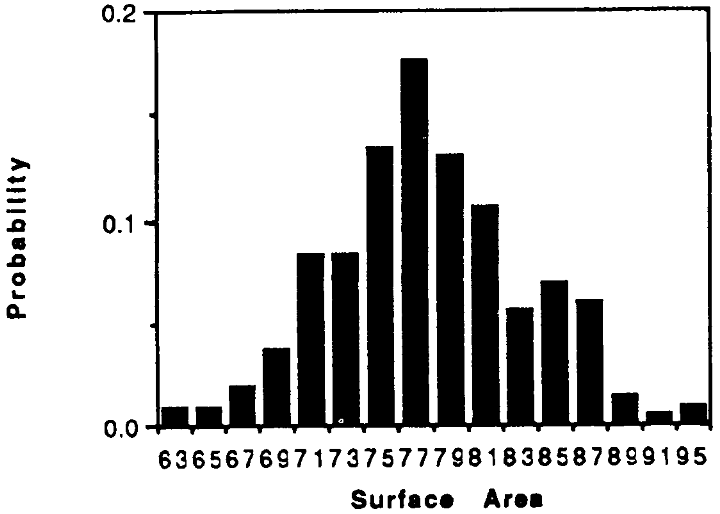

Figure 8 Distribution of the surface area (Å^2) of the faces of the Voronoi polyhedra for vitreous silica.

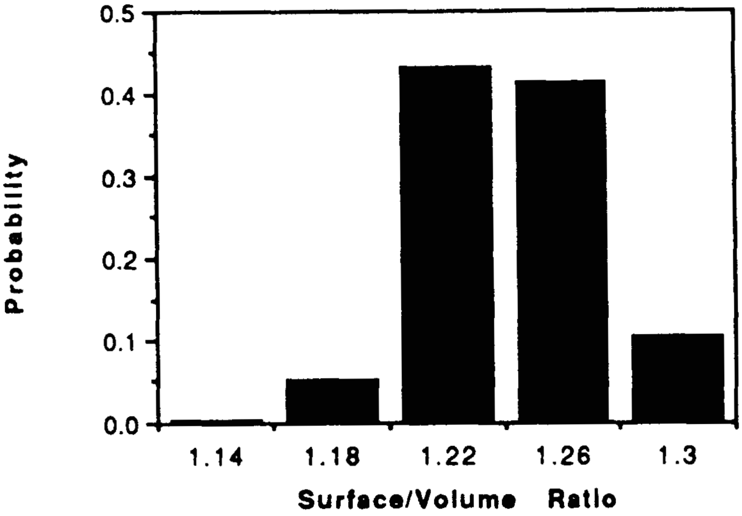

Figure 9 Surface-to-volume ratio for the Voronoi tessellation for vitreous silica.

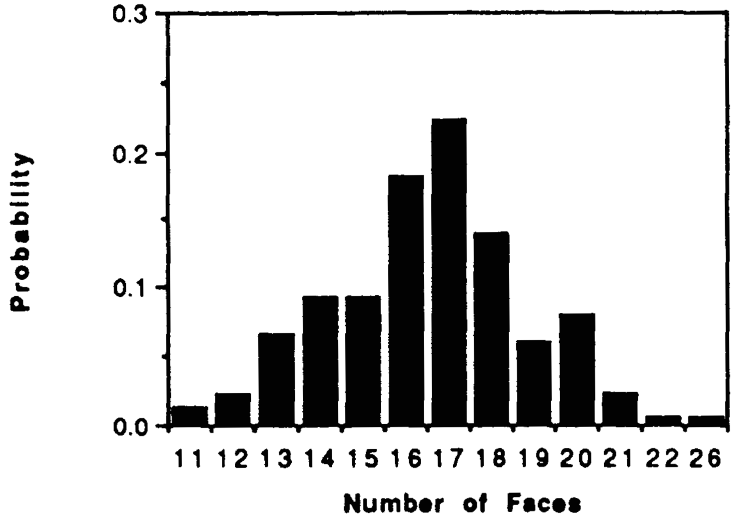

Figure 10 Distribution of the number of faces of Voronoi polyhedra for vitreous silica.

obtained by doing the Voronoi analysis on the silicon atoms only. Smaller volumes and surface areas were obtained for the polyhedra when the analysis was limited to oxygen atoms only which is not surprising because of the smaller distances between oxygen neighbors. As an example a truncated cube has eight triangular and six octagonal faces and has an ω value of 1.1771.

The value of Voronoi analysis for characterization of disordered structures has long been established. This type of analysis affords a convenient way of representing the spatial distribution of the atoms which affect the equilibrium properties of amorphous systems. Using this method each atom can be characterized by its geometric center and the shape and size of its surrounding polyhedron.

CONCLUSION

Atomistic computer simulation techniques can now provide good structural models of silica glass. Such models accord well with available experimental data.

Acknowledgments

We would like to acknowledge many useful discussions with A. C. Wright, M. Leslie and D. Rigby.

References

[1] C. R. A. Catlow and J. M. Thomas, "Modelling of catalysts and its relation to experimental problems", *Phil. Trans. Roy. Soc.*, **A341**, 255 (1992).

[2] J. A. McCammon, "Protein dynamics", *Rep. Prog. Phys.*, **47**, 1 (1984).

[3] P. Ewald, "Die Berechnung optischer und elektrostatischer Gitterpotentiale", *Ann. Physik.*, **64**, 253 (1921).

[4] M. J. L. Sangster and M. Dixon, "Interionic potentials in alkali halides and their use in simulations of the molten salts", *Advances in Physics*, **25**, 247 (1976).

[5] N. Anastasiou and D. Fincham, "Programs for the dynamic simulation of liquids and solids", *Comput. Phys. Commun.*, **25**, 159 (1982).

[6] B. Vessal, M. Leslie and C. R. A. Catlow "Molecular dynamics simulation of silica glass", *Molecular Simulation*, **3**, 123 (1989).

[7] B. Vessal, M. Amini, D. Fincham and C. R. A. Catlow, "Water-like melting behaviour of SiO_2 investigated by the molecular dynamics simulation technique", *Phil. Mag. B*, **60**, 753 (1989).

[8] B. Vessal, M. Amini, C. R. A. Catlow and M. Leslie, "Simulation studies of silicate glasses", *Trans. Am. Cryst. Assoc.*, **27**, 15 (1991).

[9] R. J. Hemley, A. P. Jephcoat, H. K. Mao, L. C. Ming and M. H. Manghnani, "Pressure-induced amorphization of crystalline silica", *Nature*, **334**, 52 (1988).

[10] C. R. A. Catlow, C. M. Freeman, B. Vessal, S. M. Tomlinson and M. Leslie, "Molecular dynamics studies of hydrocarbon diffusion in zeolites", *J. Chem. Soc. Faraday Trans.*, **87**, 1947 (1991).

[11] M. Kawano, B. Vessal and C. R. A. Catlow, "A molecular dynamics simulation of the temperature dependence of the diffusion of methane in silicalite", *J. Chem. Soc. Chem. Commun*, **879** (1992).

[12] B. Vessal, G. N. Greaves, P. T. Marten, A. V. Chadwick, R. Mole and S. Houde-Walter, "Cation microsegregation and ionic mobility in mixed alkali glasses", *Nature* **356**, 504 (1992).

[13] B. Vessal, unpublished results.

[14] B. Vessal and J. E. Dickinson, "Simulation studies of titanium and zirconium wadeite glasses", *Mater Res. Soc. Proc.*, **321**, 129 (1994).

[15] B. Vessal, M. Amini and H. Akbarzadeh, "Molecular dynamics simulation of molten silica at high pressure", *J. Chem. Phys.*, **101**, 7823 (1994).

[16] B. Vessal, M. Amini and C. R. A. Catlow, "Computer simulation of the structure of silica glass", *J. Non-Cryst. Solids*, **159**, 184 (1993).

[17] D. I. Grimley, A. C. Wright and R. N. Sinclair, "Neutron scattering from vitreous silica, IV. Time-of-flight diffraction", *J. Non-Cryst. Solids*, **119**, 49 (1990).

[18] A. C. Wright, "The comparison of molecular dynamics simulations with diffraction experiments", *J. Non-Cryst. Solids*, **159**, 264 (1993).

[19] R. J. Bell and P. Dean, "The structure of vitreous silica: Validity of the random network theory", *Phil. Mag.*, **25**, 1381 (1972).

[20] F. L. Galeener, "Planar rings in vitreous silica", *J. Non-Cryst. Solids*, **49**, 53 (1982).

[21] J. D. Kubicki and D. Sykes, "Molecular orbital calculations of vibrations in three-membered aluminosilicate rings", *Phys. Chem. Minerals*, **19**, 381 (1993).

[22] M. Tanemura, T. Ogawa and N. Ogita, "A new algorithm for three-dimensional Voronoi tessellation", *J. Comp. Phys.*, **51**, 191 (1983).

[23] A. C. Wright, B. Bachra, T. M. Brunier, R. N. Sinclair, L. F. Gladden and R. L. Portsmouth, *J. Non-Cryst. Solids*, **150**, 69 (1992).